# A Response Surface Methodology Study: Effects of Trivalent $Cr^{3+}$ Metal Ion-Catalyzed Hydrolysis on Nanocellulose Crystallinity and Yield

You Wei Chen, Hwei Voon Lee,* and Sharifah Bee Abd Hamid

The preparation of nanocellulose *via* $Cr(NO_3)_3$-assisted sulfuric acid hydrolysis was optimized using response surface methodology (RSM). The experiment was performed using a five-level, four-factor central composite design coupled with RSM in order to optimize nanocellulose crystallinity and product yield. Four factors were evaluated for the preparation of nanocellulose: (1) reaction temperature, (2) hydrolysis time, (3) $Cr(NO_3)_3$ concentration, and (4) $H_2SO_4$ concentration. Based on the RSM model, the maximum yield and highest crystallinity of nanocellulose was obtained under hydrolysis conditions of 82.2 °C, 0.22 M $Cr(NO_3)_3$, and 0.80 M $H_2SO_4$ with 1 h of reaction. Furthermore, the physicochemical properties of the obtained nanocellulose were examined, revealing that the amorphous regions were successfully hydrolyzed, while the crystalline region remained unaltered. Morphology analysis also showed that the nanocellulose was an interconnected web-like network. Thus, both $H_2SO_4$ and Cr(III) metal salt concentration were important factors that influenced the nanocellulose yield and crystallinity index.

*Keywords: Response surface methodology; Central composite design; Cr(III)-catalyzed hydrolysis; Crystallinity; Optimization*

*Contact information: Nanotechnology & Catalysis Research Centre (NANOCAT), Institute of Postgraduate Studies, University of Malaya, 50603 Kuala Lumpur, Malaysia;*
** Corresponding author: leehweivoon@um.edu.my*

## INTRODUCTION

Nanocellulose, often referred to as nanocrystalline cellulose (NCC), nanofibrillated cellulose (NFC), or bacterial nanofiber (BNF), has recently become an interesting nano-scale biomaterial that possesses excellent properties such as high surface area, high aspect ratio, high tensile strength and modulus, low density, recyclability, and biodegradability (Liu *et al.* 2010; Li *et al.* 2012). These noteworthy characteristics make nanocellulose beneficial as an advanced composite material and useful in electronic devices and textiles (Pandey *et al.* 2010).

When cellulosic materials are subjected to either chemical treatment or a combination of mechanical and chemical treatments, nanocellulose can be obtained by solubilizing the disordered arrangement of amorphous regions in the cellulose while retaining the highly organized crystalline structure (Hamid *et al.* 2015). Typically, concentrated organic acids (*e.g.*, $H_2SO_4$ (Liew *et al.* 2016), HCl (Boujemaoui *et al.* 2015), and $HNO_3$ (Azeredo *et al.* 2015)) have been used to prepare nanocellulose *via* hydrolysis of cellulose-based raw material. During hydrolysis, the amorphous regions of cellulosic material are disintegrated by hydrolytic cleavage of the glycosidic bond, but the highly ordered cellulose segments remain, with different degrees of crystallinity (Guo *et al.* 2012).

However, strong acid hydrolysis of cellulose may lead to uncontrollable depolymerization of cellulose chains into unfavourable side products, especially simple sugar monomers (glucose) rather than cellulose in solid crystalline nanoparticles, as well as side formation of by-products (humic acid) due to further polymerization of the produced sugar monomer (Kristensen *et al.* 2008). These reactions can lead to a lower product yield, aspect ratio (length/diameter ratio), and crystalline index of the nanocellulose product, which limit its application in several industrial fields (Kristensen *et al.* 2008). Therefore, the challenge of preparing highly selective and crystalline nanocellulose *via* chemical hydrolysis is a major concern.

Inorganic salts (transition metal salts) such as $FeSO_4$, $FeCl_2$, $FeCl_3$, $CuCl_2$, and $Fe(SO_4)_3$ can be utilized in the acid hydrolysis process (Peng *et al.* 2010). Inorganic salts replace mineral acid for partial depolymerization of cellulose into nanocellulose intermediates, as they are less acidic and corrosive and also create less severe conditions and environmental impact than strong mineral acids (Kristensen *et al.* 2008). $Fe^{3+}$ ion catalysts improve the acid hydrolysis of cellulose by HCl (Li *et al.* 2013). In the preparation of nanocellulose by metal salt ($FeSO_4$)-catalyzed HCl acid hydrolysis, a reaction temperature above 90 °C for 4 to 6 h created optimum conditions (Hamid *et al.* 2014; Karim *et al.* 2014). The effect of a modified transition metal salt on the hydrolytic cleavage of cellulose polymers into nanoscale fibers has been studied (Yahya *et al.* 2015). Cellulose nanofiber can also be produced *via* Ni(II)-transition metal salt hydrolysis in the absence of mineral acid; when raw microcrystalline cellulose (MCC) is treated with 1 M of $Ni(NO_3)_2$ metal salt, the optimized nanofiber product has a crystallinity index of 80.75% (Yahya *et al.* 2015). Thus, transition metal salts enhance acid hydrolysis through their strong catalytic effects. However, to decrease costs for industrial usage, a shorter hydrolysis period and/or lower concentration of metal salt catalyst is preferable. Therefore, a modified hydrolysis pretreatment for large-scale production with milder reaction conditions has been explored in this study; this modified approach combines Cr(III)-based metal salt and dilute $H_2SO_4$. Dilute $H_2SO_4$ swells and opens cellulose fibers without degrading the polymers into undesirable by-products (*i.e.*, glucose monomers) (Olsson and Westman 2013). Thus, it is possible to enhance the targeted hydrolysis of glycosidic linkages, such that long polymeric chains of cellulose are broken into nano-dimensional crystalline cellulose particles (Kopania *et al.* 2012).

In the present study, a trivalent ($Cr^{3+}$) chromium-based transition metal salt was selected as a hydrolyzing agent for the selective depolymerization of raw cellulose material into nanoparticles in the presence of dilute sulfuric acid. Cellulose and/or glucose can be converted into various useful important chemicals, *i.e.*, polyols, acids, and furans, in a metal salt-catalyzed reaction. Cr-based metal salt catalysts such as $CrCl_2$ and $CrCl_3$ are uniquely effective in hydrolyzing long polymeric chains (such as cellulose or glucose) into simpler monomer structures (such as HMF and lactic acid). Approximately 70% of glucose can be converted into HMF using 6 mol% $CrCl_2$ at 80 °C for 3 h (Zhao *et al.* 2007). In addition, Peng *et al.* (2010) reported on the use of $CrCl_3$ for the conversion of cellulose into lactic acid, showing that almost 67 mol% of the cellulose was hydrolyzed into lactic acid at 200 °C for 3 h under hydrothermal conditions. Based on these previous reports, a Cr-based metal salt catalyst is highly effective in the cleavage of glycosidic linkage of polymeric chains. Therefore, it is believed that an intermediate product (nanocellulose) could be produced *via* Cr(III)-catalyzed dilute $H_2SO_4$ hydrolysis under controlled hydrolysis conditions.

This study is the first to prepare nanocellulose *via* Cr-catalyzed hydrolysis. Thus, the aims of this study were: (i) to prepare nanocellulose *via* $Cr(NO_3)_3$ transition metal salt-assisted $H_2SO_4$ hydrolysis; (ii) to investigate the effect of reaction temperature, hydrolysis time, $Cr(NO_3)_3$ metal salt concentration, and $H_2SO_4$ concentration on the nanocellulose yield and its crystallinity index using response surface methodology (RSM); and (iii) to examine the physicochemical properties of the obtained nanocellulose in terms of crystallinity, structure, morphology, and particle size.

## EXPERIMENTAL

### Materials

Alpha cellulose (Sigma-Aldrich, USA) was used as the raw material. Concentrated sulfuric acid ($H_2SO_4$, 95 to 97%) and $Cr(NO_3)_3$ salt were obtained from R&M Chemicals (Malaysia). All chemicals used were analytical grade without further purification.

### Methods

*Preparation of nanocellulose*

Cellulose powder (0.6 g) was placed in a round-bottomed flask. The powder was treated with varying concentrations of $H_2SO_4$ and $Cr(NO_3)_3$ solutions at reaction temperatures between 30 and 100 °C and reaction times of 0.5 to 2.5 h under a constant stirring speed. The treated samples were washed with deionized water several times, dialyzed until the pH reached neutrality (pH 7), and then freeze-dried. The percentage of nanocellulose yield was calculated according to Eq. 1 (Abd Hamid *et al.* 2014),

$$\text{Yield (\%)} = w_o / w_t \times 100 \quad (1)$$

where $w_t$ refers to the initial weight of the cellulose sample and $w_o$ is the dry weight of the freeze-dried powder.

*Experimental design for optimization study*

The experimental design matrix, data analysis, and optimization study were developed using the software Design-Expert Expert version 9.0.0 (Stat-Ease, Inc., Minneapolis, USA). A standard RSM design called central composite design (CCD) was applied to study the Cr(III)-assisted acid hydrolysis of cellulose for the preparation of nanocellulose. The four independent variables studied were reaction temperature ($x_1$), reaction time ($x_2$), $Cr(NO_3)_3$ metal salt concentration ($x_3$), and $H_2SO_4$ concentration ($x_4$). The responses were crystallinity index ($y_1$) and nanocellulose yield ($y_2$).

Table 1 lists the range and levels of the four independent variables studied with actual and coded levels of each parameter. The independent variables were coded into two levels: namely, low (−1) and high (+1), whereas the axial points were coded as −2 (−α) and +2 (+α). In this study, the α-value was fixed at 2, which is the distance of the axial point from the center and makes the design rotatable. The experimental design matrix, in terms of real and coded independent variables and the results, is presented in Table 2. The experiments were run in random order to minimize errors from systematic trends in the variables.

**Table 1.** Five Level, Four Factor Central Composite Design of the Hydrolysis Condition Variables

| Coded Symbol | Variable | Levels | | | | |
|---|---|---|---|---|---|---|
| | | -α | -1 | 0 | +1 | +α |
| $x_1$ | Temperature (°C) | 30.0 | 47.5 | 65.0 | 82.5 | 100.0 |
| $x_2$ | Reaction time (h) | 0.5 | 1.0 | 1.5 | 2.0 | 2.5 |
| $x_3$ | $Cr(NO_3)_3$ concentration (M) | 0.025 | 0.125 | 0.225 | 0.325 | 0.425 |
| $x_4$ | $H_2SO_4$ concentration (M) | 0.2 | 0.4 | 0.6 | 0.8 | 1.0 |

**Table 2.** Experimental Design Matrix and Experimental Results for Nanocellulose Preparation *via* Cr(III)-assisted $H_2SO_4$ Hydrolysis

| Run | Variables Levels | | | | Responses | |
|---|---|---|---|---|---|---|
| | $x_1$ | $x_2$ | $x_3$ | $x_4$ | Crystallinity $y_1$ (%) | Yield $y_2$ (%) |
| 1 | 0 (65.00) | 0 (1.50) | 0 (0.225) | 0 (0.60) | 83.33 | 80.14 |
| 2 | 0 (65.00) | 0 (1.50) | 0 (0.225) | 0 (0.60) | 83.08 | 80.32 |
| 3 | 0 (65.00) | 0 (1.50) | 0 (0.225) | 0 (0.60) | 82.24 | 80.22 |
| 4 | 0 (65.00) | 0 (1.50) | 0 (0.225) | 0 (0.60) | 82.85 | 80.52 |
| 5 | 0 (65.00) | 0 (1.50) | 0 (0.225) | 0 (0.60) | 82.72 | 80.85 |
| 6 | 0 (65.00) | 0 (1.50) | 0 (0.225) | 0 (0.60) | 83.74 | 80.53 |
| 7 | 0 (65.00) | 0 (1.50) | 2 (0.425) | 0 (0.60) | 86.23 | 80.61 |
| 8 | -2 (30.00) | 0 (1.50) | 0 (0.225) | 0 (0.60) | 70.33 | 88.00 |
| 9 | 2 (100.00) | 0 (1.50) | 0 (0.225) | 0 (0.60) | 88.93 | 83.20 |
| 10 | 0 (65.00) | 2 (2.50) | 0 (0.225) | 0 (0.60) | 85.52 | 80.93 |
| 11 | 0 (65.00) | -2 (0.50) | 0 (0.225) | 0 (0.60) | 66.55 | 91.02 |
| 12 | 0 (65.00) | 0 (1.50) | 0 (0.225) | -2 (0.20) | 60.11 | 90.55 |
| 13 | 0 (65.00) | 0 (1.50) | 0 (0.225) | 2 (1.00) | 77.44 | 80.11 |
| 14 | 0 (65.00) | 0 (1.50) | -2 (0.025) | 0 (0.60) | 63.99 | 89.63 |
| 15 | -1 (47.50) | 1 (2.00) | -1 (0.125) | -1 (0.40) | 67.91 | 88.86 |
| 16 | 1 (82.50) | 1 (2.00) | 1 (0.325) | -1 (0.40) | 83.71 | 84.45 |
| 17 | 1 (82.50) | 1 (2.00) | -1 (0.125) | 1 (0.80) | 84.16 | 82.53 |
| 18 | 1 (82.50) | -1 (1.00) | 1 (0.325) | 1 (0.80) | 86.13 | 80.87 |
| 19 | -1 (47.50) | 1 (2.00) | 1 (0.325) | 1 (0.80) | 84.11 | 82.56 |
| 20 | -1 (47.50) | -1 (1.00) | 1 (0.325) | -1 (0.40) | 60.38 | 87.49 |
| 21 | 1 (82.50) | -1 (1.00) | -1 (0.125) | -1 (0.40) | 65.87 | 89.63 |
| 22 | -1 (47.50) | -1 (1.00) | -1 (0.125) | 1 (0.80) | 83.81 | 82.99 |
| 23 | -1 (47.50) | 1 (2.00) | 1 (0.325) | -1 (0.40) | 74.18 | 86.97 |
| 24 | -1 (47.50) | 1 (2.00) | -1 (0.125) | 1(0.80) | 67.09 | 88.33 |
| 25 | 1 (82.50) | 1 (2.00) | 1 (0.325) | 1 (0.80) | 88.58 | 77.19 |
| 26 | -1 (47.50) | -1 (1.00) | 1 (0.325) | 1 (0.80) | 82.48 | 81.14 |
| 27 | -1 (47.50) | -1 (1.00) | -1 (0.125) | -1 (0.40) | 62.63 | 89.27 |
| 28 | 1 (82.50) | -1 (1.00) | 1 (0.325) | -1 (0.40) | 72.35 | 85.55 |
| 29 | 1 (82.50) | 1 (2.00) | -1 (0.125) | -1 (0.40) | 74.25 | 86.38 |
| 30 | 1 (82.50) | -1 (1.00) | -1 (0.125) | 1 (0.80) | 82.81 | 85.55 |

*Product characterization*

The X-ray diffraction (XRD) data was investigated by a PANalytical Empyrean X-ray diffractometer (Netherlands) with a CuKα radiation source (λ = 0.154 nm). The XRD patterns were measured in the 2$\theta$ range of 5° to 60°. The crystalline index (*CrI*) of cellulose samples was calculated using Segal's method, as shown in Eq. 2:

$$CrI\ (\%) = (I_{002} - I_{am}) / I_{002} \times 100 \quad (2)$$

where $I_{002}$ is the overall intensity for the crystalline material at $2\theta = 22.5°$ and $I_{am}$ is the intensity at $2\theta = 18.5°$, which represents amorphous material (Segal *et al.* 1959).

The morphology of the samples was characterized by field emission scanning electron microscopy (FESEM), transmission electron microscopy (TEM), and atomic force microscopy (AFM). Platinum-coated samples were analyzed with a Hitachi SU8030 FESEM microscope (Japan) operated with an accelerating voltage of 5 kV. For TEM, a drop of diluted sample was deposited on a carbon-coated copper grid, and the microscope (Tecnai $G^2$ F20 series, USA) was operated at an acceleration voltage of 200 kV. To examine the surface morphology of the samples, tapping mode AFM was performed with a NT-MDT (Russia).

Surface functional groups of the samples were examined by Fourier transform infrared (FTIR) spectroscopy with a Bruker IFS 66 v/S FTIR spectrometer (Germany) with a range of 4000 to 400 $cm^{-1}$, a resolution of 4 $cm^{-1}$, and 64 scans.

## RESULTS AND DISCUSSION

### Model Selection and Statistical Analysis

Two regression models describing the nanocellulose yield and crystallinity index were developed. The statistical significance of the model terms was determined by analysis of variance (ANOVA). The responses were the crystallinity and yield of synthesized nanocellulose, as determined by the CCD (Table 2). The nanocellulose crystallinity ($y_1$) ranged from 60.38 to 88.93%, and the yield ($y_2$) was between 77.19 and 91.02%. The relationship between the crystallinity or nanocellulose yield and the four independent variables was calculated by Eqs. 3 and 4, which are expressed using the coded factors (Table 1).

Crystallinity index (3)

$$y_1 = 82.99 + 3.85\,x_1 + 2.73\,x_2 + 3.66\,x_3 + 5.52\,x_4 + 1.22\,x_1x_2 + 0.25\,x_1x_3 - 0.43\,x_1x_4 + 1.93\,x_2x_3 - 3.13\,x_2x_4 + 0.22\,x_3x_4 - 0.61\,x_1^2 - 1.51\,x_2^2 - 1.74\,x_3^2 - 3.32\,x_4^2$$

Nanocellulose yield (4)

$$y_2 = 80.43 - 1.04\,x_1 - 1.06\,x_2 - 1.89\,x_3 - 2.43\,x_4 - 1.06\,x_1x_2 - 0.30\,x_1x_3 - 0.14\,x_1x_4 - 0.16\,x_2x_3 + 0.33\,x_2x_4 - 0.50\,x_3x_4 + 1.21\,x_1^2 + 1.30\,x_2^2 + 1.09\,x_3^2 + 1.14\,x_4^2$$

where $y_1$ is the crystallinity index and $y_2$ is the yield of nanocellulose; $x_1$, $x_2$, $x_3$, and $x_4$ are the independent variables for reaction temperature, reaction time, Cr(III) metal ion concentration, and $H_2SO_4$ concentration, respectively.

The regression coefficients of both developed response surface models, corresponding $R^2$ values, mean, coefficient of variation (CV), and adequate precision are provided in Table 3. It was observed that the CV value for the models of crystallinity index and nanocellulose yield was 5.09 and 2.06, respectively, which implied that there was a high degree of precision and a good deal of reliability of the experimental values in the reaction models. Moreover, the small value of standard deviation (SD) for both responses ($y_1$ and $y_2$) at 3.94 and 1.73, respectively, indicated good precision, reproducibility, and reliability of the experimental models (Li *et al.* 2014). The precision of the model reflects

the signal-to-noise ratio, and a value larger than 4 is normally desirable (Karim *et al.* 2014). The obtained precision values of 11.224 and 10.433 for crystallinity index and nanocellulose yield models, respectively. The obtained adequate precision values for both models were well above 4, which indicates an adequate signal, and further suggests that the proposed models can be used to navigate the design space (Hamid *et al.* 2014; Karim *et al.* 2014; Mohan *et al.* 2014).

The ANOVA for the Cr(III)-assisted hydrolysis model of the response surface of crystallinity index ($y_1$) and nanocellulose yield ($y_2$) is shown in Tables 4 and 5, respectively. Based on the obtained data, the value of probable *F* for both responses, $y_1$ and $y_2$, was less than 0.0001. This result was highly significant because there was only a 0.01% chance that a model *F* value of this magnitude could occur due to noise (Feng *et al.* 2015). Furthermore, the prob > *F* value for the variables ($x_1$, $x_2$, $x_3$, and $x_4$) in both quadratic models (crystallinity index and nanocellulose yield) was smaller than 0.05, which meant that the model was significant in terms of both responses ($y_1$ and $y_2$). In addition, the reaction variable of $H_2SO_4$ concentration had the greatest effect on both responses, which exhibited the highest *F* values of 732.21 and 141.68, respectively.

**Table 3.** Statistical Parameters for ANOVA Analysis of Crystallinity Index ($Y_1$) and Nanocellulose Yield ($Y_2$) Model Regressions

| Statistical Parameters | Percentage of Crystallinity, $y_1$ | Percentage of Yield, $y_2$ |
|---|---|---|
| Standard deviation (SD %) | 3.95 | 1.73 |
| R-squared ($R^2$) | 0.9157 | 0.9138 |
| Mean | 77.25 | 84.21 |
| Coefficient of variation (CV) | 5.11 | 2.06 |
| Adequate precision | 11.224 | 10.433 |

**Table 4.** ANOVA Study for Crystallinity Index ($Y_1$) Model Regression

| Source | Sum of Squares | Degree of Freedom | Mean Square | *F* value | Prob > *F* |
|---|---|---|---|---|---|
| Model | 2203.6 | 14 | 157.4 | 10.09 | < 0.0001 |
| $x_1$ | 356.20 | 1 | 356.2 | 22.83 | 0.0004 |
| $x_2$ | 178.65 | 1 | 178.65 | 11.45 | 0.0049 |
| $x_3$ | 321.51 | 1 | 321.51 | 20.61 | 0.0006 |
| $x_4$ | 732.21 | 1 | 732.21 | 46.94 | < 0.0001 |
| $x_1x_2$ | 23.86 | 1 | 23.86 | 1.53 | 0.2380 |
| $x_1x_3$ | 0.99 | 1 | 0.99 | 0.063 | 0.8051 |
| $x_1x_4$ | 2.98 | 1 | 2.98 | 0.19 | 0.6695 |
| $x_2x_3$ | 59.83 | 1 | 59.83 | 3.84 | 0.0720 |
| $x_2x_4$ | 156.88 | 1 | 156.88 | 10.06 | 0.0074 |
| $x_3x_4$ | 0.75 | 1 | 0.75 | 0.048 | 0.8300 |
| $x_1^2$ | 10.15 | 1 | 10.15 | 0.65 | 0.4343 |
| $x_2^2$ | 62.39 | 1 | 62.39 | 4.00 | 0.0669 |
| $x_3^2$ | 82.88 | 1 | 82.88 | 5.31 | 0.0383 |
| $x_4^2$ | 302.8 | 1 | 302.8 | 19.41 | 0.0007 |

**Table 5.** ANOVA Study for Nanocellulose Yield ($Y_2$) Model Regression

| Source | Sum of Squares | Degree of Freedom | Mean Square | *F* value | Prob > *F* |
|---|---|---|---|---|---|
| Model | 414.36 | 14 | 29.60 | 9.84 | < 0.0001 |
| $x_1$ | 26.19 | 1 | 26.19 | 8.71 | 0.0112 |
| $x_2$ | 26.88 | 1 | 26.88 | 8.94 | 0.0104 |
| $x_3$ | 85.74 | 1 | 85.74 | 28.52 | 0.0001 |
| $x_4$ | 141.68 | 1 | 141.68 | 47.12 | < 0.0001 |
| $x_1x_2$ | 17.82 | 1 | 17.82 | 5.93 | 0.0301 |
| $x_1x_3$ | 1.4 | 1 | 1.4 | 0.47 | 0.5070 |
| $x_1x_4$ | 0.33 | 1 | 0.33 | 0.11 | 0.7456 |
| $x_2x_3$ | 0.4 | 1 | 0.4 | 0.13 | 0.7206 |
| $x_2x_4$ | 1.79 | 1 | 1.79 | 0.59 | 0.4545 |
| $x_3x_4$ | 3.97 | 1 | 3.97 | 1.32 | 0.2714 |
| $x_1^2$ | 39.87 | 1 | 39.87 | 13.26 | 0.0030 |
| $x_2^2$ | 46.31 | 1 | 46.31 | 15.4 | 0.0017 |
| $x_3^2$ | 32.33 | 1 | 32.33 | 10.75 | 0.0060 |
| $x_4^2$ | 35.54 | 1 | 35.54 | 11.82 | 0.0044 |

*Prof > F value less than 0.05 designates that model terms are significant

Figure 1 shows the linear plots of predicted *versus* actual percentage for the models of crystallinity index and nanocellulose yield. The coefficient of determination ($R^2$) value should be higher than 0.8000 for a well-fitted model (Hamid *et al.* 2014). Based on these two plots, the $R^2$ value of crystallinity index model was 0.9157, and the $R^2$ value for nanocellulose yield model was 0.9138. Because the predicted values were close to 1, the models were accurate in estimating responses in the range studied (Tang *et al.* 2011; Karim *et al.* 2014).

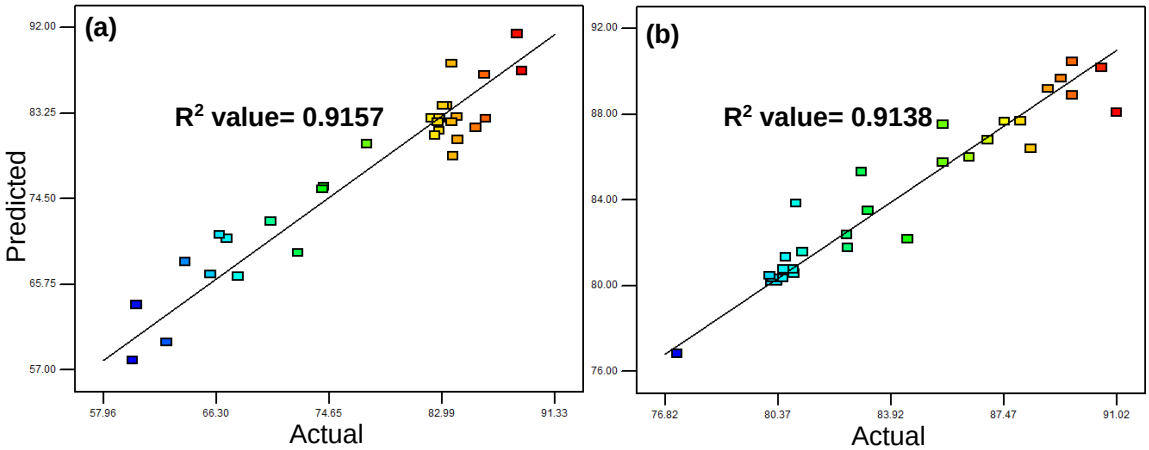


**Fig. 1.** Predicted *versus* actual plots (a) crystallinity index, and (b) nanocellulose yield

## Effect of Hydrolysis Variables by RSM Optimization Study

Of the four variables including reaction temperature ($x_1$), reaction time ($x_2$), Cr(III) metal salt concentration ($x_3$), and $H_2SO_4$ concentration ($x_4$), RSM predicted that the $H_2SO_4$ concentration ($x_4$) and Cr(III) metal salt concentration ($x_3$) had the greatest influence on the crystallinity index and nanocellulose yield. Generally, the effect of the interaction between two hydrolysis variables is demonstrated by response surface plots, while the other variables are kept at zero.

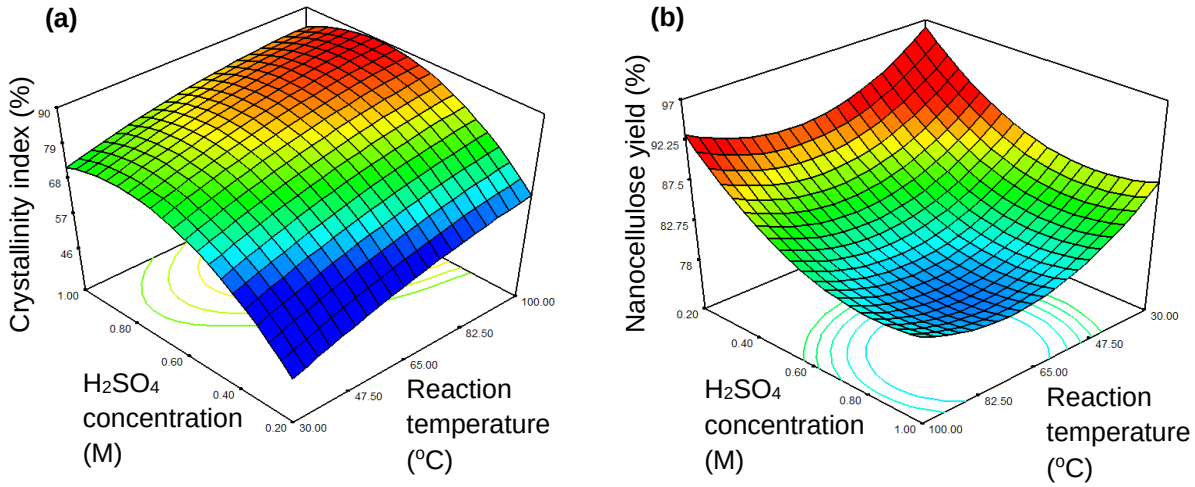


**Fig. 2.** Interaction between reaction temperature ($x_1$) and $H_2SO_4$ concentration ($x_4$), with a fixed reaction time ($x_2$) of 1.5 h and $Cr(NO_3)_3$ concentration ($x_3$) of 0.23 M. (a) crystallinity index model and (b) nanocellulose yield model

Figure 2 shows 3-D plots of the interaction between reaction temperature and $H_2SO_4$ concentration and the corresponding effects on the crystallinity index and nanocellulose yield. The reaction time and $Cr(NO_3)_3$ metal salt concentration were fixed at 1.5 h and 0.30 M, respectively. The reaction temperature played an important role by initiating and enhancing the chemical degradation of cellulose material. The 3-D response surface shows that an increase in reaction temperature from low (30 °C) to high (100 °C) was the main parameter contributing to the increase of crystallinity index, as shown in Fig. 2a. At a low concentration of sulfuric acid (0.2 M), an increase in the reaction temperature greatly enhanced the crystallinity index of the yielded nanocellulose from 30 °C to 100 °C, but it had a negative effect at a high concentration of sulfuric acid (1.0 M) and reaction temperature (100 °C) (Fig. 2a). The decrease in the crystallinity index of the yielded nanocellulose at high sulfuric acid concentrations and high reaction temperatures was due to over-reaction. When over-reaction occurred under such extreme conditions as excessive heat energy and extensive hydrolysis time, cellulose was degraded into its simpler sugar monomers by hydrolysis (Lu *et al.* 2014).

In addition, increasing the reaction temperature from 30 °C to 100 °C did not greatly improve the crystallinity index of nanocellulose with a high sulfuric acid concentration (1.0 M). A possible explanation for this result is that the partial crystallite structure was damaged by the concentrated acid when the amorphous regions of cellulose matrix were degraded during the hydrolysis process, even when the reaction was carried out at a low reaction temperature (Fig. 2a). Generally, this result agreed with a previous study in which increased reaction temperature and acid concentration increased the crystallinity index (Li *et al.* 2014). Therefore, the reaction conditions must be controlled in order to prevent over-degradation of cellulose into undesirable products.

The simultaneous dependence of nanocellulose yield on the reaction temperature and sulfuric acid concentration is shown in Fig. 2b. In a reaction time of 1.5 h, the 3-D surface plot revealed that an increase in reaction temperature and amount of sulfuric acid caused a significant decrease of nanocellulose yield (96 to 87%) at a low reaction temperature (30 °C). The reduction in nanocellulose yield was higher at 100 °C, in which the nanocellulose yield declined from 93 to 82%. This result might indicate that more

hydrogen bonds were broken at such a high reaction temperature, which led to more cellulose degradation into water-soluble glucose monomers. This finding was in accordance with a previous study (Abd Hamid *et al.* 2014).

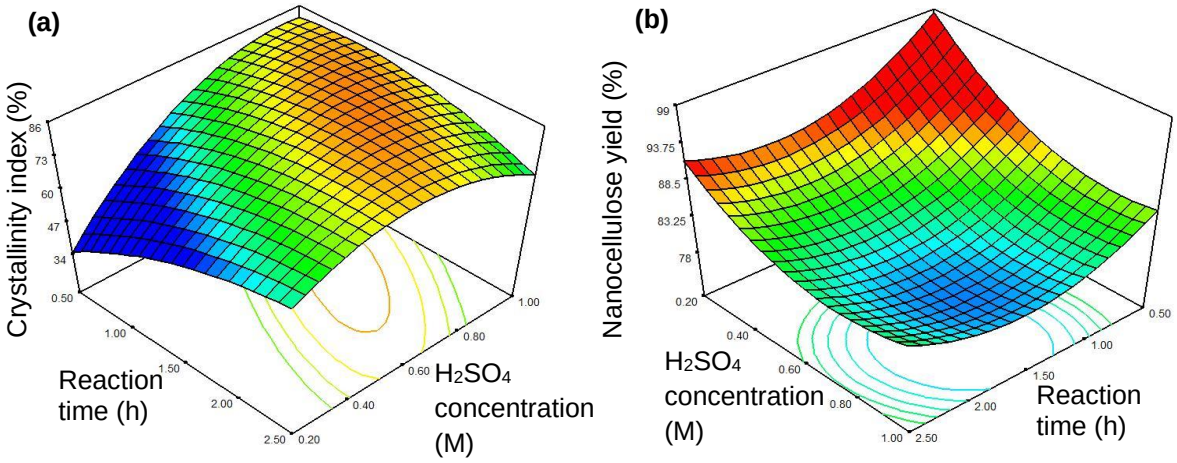


**Fig. 3.** Interaction between reaction time ($x_2$) and $H_2SO_4$ concentration ($x_4$), with a fixed reaction temperature ($x_1$) of 65 °C and $Cr(NO_3)_3$ concentration ($x_3$) of 0.23 M. (a) crystallinity index model and (b) nanocellulose yield model

The effect of reaction time and sulfuric acid concentration on the produced nanocellulose crystallinity index and the yield (reaction temperature and $Cr(NO_3)_3$ concentration were kept constant at 65 °C and 0.23 M) is shown in Fig. 3. With a reaction temperature of 65 °C, the 3-D surface plot showed that an increase in reaction time caused a significant increase in nanocellulose crystallinity index (37 to 72%) at low levels of sulfuric acid concentration (0.2 M). However, the crystallinity index of yielded nanocellulose was slightly influenced by prolonging the reaction time from 0.5 h to 1.0 h at high concentrations of sulfuric acid (1.0 M), as the increment of the crystallinity index was low (83 to 85 %). However, further progress of the hydrolysis reaction caused the negative effect in enhancing the crystallinity index, as the over-degradation of cellulose polymeric chain occurred under strong acidic condition, resulted in reducing the crystallinity of obtained nanocellulose (Fig. 3a). Reaction time plays an important role in cellulose depolymerization. In the initial step, increasing contact time (hydrolysis time) was necessary in order to let more acids and metal ion catalysts diffuse into the amorphous regions of cellulose and cause the physical swelling of cellulose (Abd Hamid *et al.* 2014). Thus, the cellulose matrix was softened, and glycosidic linkages of cellulose fibers were solubilized until an optimal condition was achieved. However, further increases in reaction time and sulfuric acid concentration did not significantly increase the crystallinity index of the yielded nanocellulose. The complete dissolution of amorphous regions occurred in high concentrations of catalyst, and the crystallite regions were damaged by hydrolysis catalysts at higher reaction temperatures. Eventually the ordered structure of cellulose fiber was reduced, decreasing the crystallinity index of yielded nanocellulose. Prolonging the reaction time could further enhance the crystallinity index of obtained nanocellulose; however, the hydrolysis time must be controlled to minimize over-depolymerization hydrolysis of cellulose (Zhao *et al.* 2011). Abd Hamid *et al.* (2014) discouraged increasing the reaction time to produce nanocellulose, as it might decrease the nanocellulose crystallinity and yield (Abd Hamid *et al*. 2014).

For the nanocellulose yield reaction model, the 3-D surface plot in Fig. 3b showed that an increment of reaction time at a high sulfuric acid concentration did not cause significant changes in nanocellulose yield as compared with a low amount of sulfuric acid. This result reflects the fact that the majority of cellulose was degraded into glucose monomer at an early reaction time (0.5 h) under strong acid hydrolysis (1.0 M). In the case of sulfuric acid concentration, the contour plot showed that the nanocellulose yield decreased gradually at a short reaction time with a continuously increasing amount of sulfuric acid. At a long reaction time (2.5 h), the nanocellulose yield was reduced from 91 to 84% at 65 °C with 0.23 M of $Cr(NO_3)_3$ metal salt catalyst. However, the response surface plot indicated that both individual factors (reaction time and sulfuric acid concentration) had negative effects on the yield of hydrolyzed nanocellulose. The model demonstrated that increased sulfuric acid concentration resulted in a marginal decrease of nanocellulose yield for different hydrolysis times. However, the lowest nanocellulose yield (77.19%) was obtained when the hydrolysis reaction was conducted at a high temperature of 82.50 °C for 2 h with a high catalyst loading of 0.325 M $Cr(NO_3)_3$ and 0.80 M sulfuric acid (Sample 25), which reflected the chemical degradation of cellulose polymers.

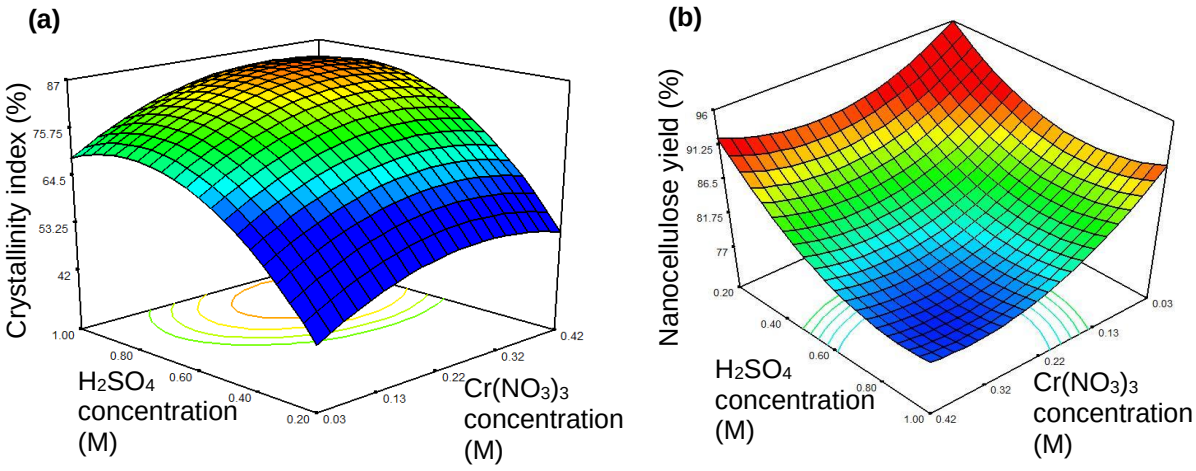


**Fig. 4.** Interaction between $Cr(NO_3)_3$ concentration ($x_3$) and $H_2SO_4$ concentration ($x_4$), with a fixed reaction temperature ($x_1$) of 65 °C and reaction time ($x_2$) of 1.5 h. (a) crystallinity index model and (b) nanocellulose yield model

Figure 4 illustrates the surface contour plot for the effect of sulfuric acid concentration and $Cr(NO_3)_3$ metal salt on the crystallinity index and yield of produced nanocellulose. The reaction temperature and hydrolysis time were fixed at 65 °C and 1.5 h, respectively. The interaction between these two individual factors created a dome shape, in which the crystalline index of yielded cellulose increased gradually to a certain level, followed by a decrease with higher catalyst loading. This decline indicated that the majority of the amorphous regions of cellulose were hydrolyzed. The crystallite regions were left unaltered at the optimum time, and further increasing the amount of catalyst led to over-degradation of cellulose, facilitating the disintegration of the cellulosic fiber into glucose monomers. The partial elliptical contour plot (Fig. 4a) indicated that the $Cr(NO_3)_3$ metal salt catalyst greatly enhanced the crystallinity index of nanocellulose. With increasing $Cr(NO_3)_3$ metal salt catalyst at a low concentration of sulfuric acid (0.2 M), the change in crystallinity index was dramatic (45 to 60.12%). As expected, when increasing the concentration of hydrolysis catalyst ($H_2SO_4$ or $Cr(NO_3)_3$), the yield of nanocellulose was

eventually decreased by the chemical degradation of cellulose in the acid hydrolyzing medium.

As shown in Eqs. 5 through 8, Cr(III) ions form a coordination complex with $H_2O$ to yield hydronium ions ($H_3O^+$), which further enhanced the acidity of the medium, resulting in the disintegration of hydrogen bonds between cellulose polymeric chains as well as the hydrolytic cleavage of glycosidic bonds between glucose units. Furthermore, the $Cr^{3+}$ metal ions were absorbed onto the oxygen atoms of the glucose unit in cellulose to form intermediate complexes. This interaction lowers the activation energy of hydrolysis by increasing the pyranose bond length and its bond angle (Zhao *et al.* 2011). Thus, the metal ion catalyst could further enhance the efficiency of hydrolysis.

$$Cr(NO_3)_3 + 6H_2O \rightarrow [Cr(H_2O)_6]^{3+} + 3NO_3^- \quad (5)$$

$$[Cr(H_2O)_6]^{3+} + H_2O \rightarrow [Cr(H_2O)_5(OH)]^{2+} + H_3O^+ \quad (6)$$

$$[Cr(H_2O)_5(OH)]^{2+} + H_2O \rightarrow [Cr(H_2O)_4(OH)_2]^{+} + H_3O^+ \quad (7)$$

$$[Cr(H_2O)_4(OH)_2]^{2+} + H_2O \rightarrow [Cr(H_2O)_3(OH)_3] + H_3O^+ \quad (8)$$

## Verification and Optimization of the Predictive Model

The nanocellulose synthesis process was optimized to generate the highest crystallinity index and the maximum product yield. The independent variables (reaction temperature, reaction time, $Cr(NO_3)_3$ metal salt concentration, and $H_2SO_4$ concentration) were set in low and high levels that were coded as -2 and +2, respectively, while the responses (crystallinity index and nanocellulose yield) were set at the maximum point.

However, the economic feasibility of acid hydrolysis operation was considered. The main concerns were moderate reaction temperature and reaction time, low quantities of $Cr(NO_3)_3$, and low $H_2SO_4$ concentrations. Although the reaction temperature and hydrolysis time had a positive impact on the crystallinity index of nanocellulose, these parameters needed to be maintained in moderate conditions to minimize the required production energy. To reduce production costs, only the minimally adequate amounts of the hydrolysis catalysts ($Cr(NO_3)_3$ metal salt and $H_2SO_4$ acid) should be used.

**Table 6.** Predicted and Experimental Values in Optimum Preparation Conditions

| Temperature (°C) | Time (h) | $Cr(NO_3)_3$ (M) | $H_2SO_4$ (M) | Crystallinity Index (%) | | Nanocellulose Yield (%) | |
|---|---|---|---|---|---|---|---|
| | | | | Actual | Predicted | Actual | Predicted |
| 82.2 | 1.0 | 0.21 | 0.80 | 84.63 | 85.45 | 81.69 | 82.59 |
| 82.5 | 1.0 | 0.23 | 0.80 | 86.63 | 85.90 | 83.67 | 82.17 |
| 81.9 | 1.0 | 0.21 | 0.80 | 84.78 | 85.52 | 83.21 | 82.49 |

To verify the models, the optimal reaction conditions were applied to three independent replicates of the Cr(III)-catalyzed acid hydrolysis reaction (Table 6) with the following optimized conditions: reaction temperature, 82.2 °C; reaction time, 1 h; $Cr(NO_3)_3$ concentration, 0.22 M; and $H_2SO_4$ concentration, 0.80 M. Under the optimized conditions, the experimental (actual) results for crystallinity index and nanocellulose yield were 85.35% and 82.86%, respectively, which were close to the predicted values (85.62 and 82.42%). The small error (0.316 and 0.513%) indicated that the developed model was reasonably accurate. In addition, the optimal crystallinity index of yielded nanocellulose

was higher than previously reported, ranging from 63.6 to 83.5% (Table 7). This result suggested that the mild hydrolysis conditions and high selectivity for cleavage of glycosidic linkages led to the degradation of the cellulose amorphous region. This effect eventually minimized the possibility of over-depolymerization of cellulose and the formation of undesirable products (glucose monomers).

**Table 7.** Comparison of Crystallinity Index and Nanocellulose Yield

| Raw Material | Optimal Hydrolysis Conditions | Crystallinity Index (%) | Nanocellulose Yield (%) | Reference |
|---|---|---|---|---|
| PTC cellulose | 97.9 °C, 4.0 h, 0.8 M $FeCl_3$, 3.0 M HCl | 68.66 | 83.98 | (Abd Hamid *et al.* 2014) |
| Microcrystalline cellulose | 91.0 °C, 6.0 h, 1.0 M $FeCl_3$, 2.5 M HCl | 83.46 | 86.98 | (Karim *et al*. 2014) |
| *Eucalyptus* pulp | 88.3 °C, 1.1 h, 0.4 M $FeCl_3$, 2.46 M HCl | 63.59 | - | (Li *et al.* 2014) |
| *Eucalyptus* pulp | 80.0 °C, 1.2 h, 0.3 M $FeCl_3$, 2.50 M HCl | 69.50 | - | (Li *et al.* 2015) |
| Alpha cellulose | 82.2 °C, 1.0 h, 0.22 M $Cr(NO_3)_3$, 0.80 M $H_2SO_4$ | 85.35 | 82.86 | This study |

At the same temperature (82.2 °C), hydrolysis time (1 h), and $H_2SO_4$ concentration (0.8 M), the experiment was carried out without $Cr(NO_3)_3$. The crystallinity index (CrI) of the nanocellulose was only 72.24%, which was lower than nanocellulose prepared with both $H_2SO_4$ and $Cr(NO_3)_3$ metal salt. Thus, $Cr(NO_3)_3$ enhanced the nanocellulose crystallinity by 18.15%; the purpose of this experiment was to ascertain whether the presence of $Cr(NO_3)_3$ metal salt catalyst enhanced the hydrolytic cleavage of cellulose amorphous regions that correspond to higher crystallinity percentage. Moreover, this finding also suggested that dilute $H_2SO_4$ acid alone was not effective in degrading cellulose amorphous regions and breaking the intermolecular and intramolecular bonding of cellulose. The dilute $H_2SO_4$ was only capable of swelling and opening the cellulose fibers without further degradation (Kopania *et al.* 2012). A similar observation was reported by Li *et al.* (2013), in which acid hydrolysis was enhanced by the addition of metal salt, resulting in a higher crystallinity of nanocellulose.

A similar experiment was performed using the optimal conditions of temperature, time, and metal salt concentration (Table 6) in the presence of HCl (0.8 M) instead of $H_2SO_4$. These results are summarized in Table 8. The crystallinity index of yielded HCl-treated nanocellulose was only 65.52%, indicating that HCl is a weaker acid with fewer dissociated protons than $H_2SO_4$. Therefore, fewer hydronium ($H_3O^+$) ions were available to cleave the intra- and intermolecular hydrogen bonds of the cellulose polymers.

**Table 8.** Nanocellulose Crystallinity Index Obtained by Different Reactions

| Nanocellulose Sample | Temp. (°C) | Time (h) | $Cr(NO_3)_3$ conc. (M) | $H_2SO_4$ conc. (M) | HCl conc. (M) | CrI (%) |
|---|---|---|---|---|---|---|
| RSM-optimized | 82.2 | 1.0 | 0.16 | 0.80 | - | 85.35 |
| HCl-treated | 82.2 | 1.0 | 0.16 | - | 0.80 | 65.52 |
| Hydrolyzed without metal salt | 82.2 | 1.0 | - | 0.80 | - | 72.24 |

## Physicochemical Properties of Cellulose Raw Material and Cr(III)-treated Nanocellulose

*Crystallinity study and XRD analysis*

The crystallinity of the cellulose and RSM-optimized nanocellulose was studied by wide-angle X-ray diffraction (WAXRD) (Fig. 5). The similar XRD patterns for both raw material and product indicated that the chemical structure of nanocellulose remained unchanged after catalytic acid hydrolysis. Moreover, the peak intensity around $2\theta = 22.5°$ for the nanocellulose product was higher and sharper than cellulose. This result showed that most of the amorphous regions in treated nanocellulose were selectively degraded, whereas the well-ordered organized crystallite regions in fiber remained after the hydrolysis reaction. Therefore, the crystallinity index of nanocellulose (85.35%) increased sharply compared with raw cellulose (45.82%).

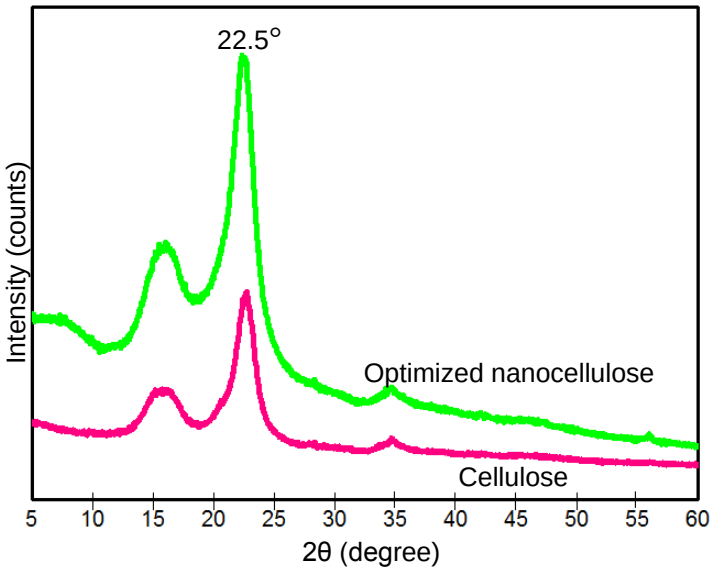


**Fig. 5.** XRD patterns of cellulose raw material and optimized nanocellulose

*Morphology and microstructure: FESEM, AFM, and TEM analyses*

The morphology and fiber structure of cellulose raw material and Cr(III)-treated nanocellulose were determined by FESEM, TEM, and AFM (Fig. 6). As shown in Fig. 6a, the cellulose fibers exhibited a compact and aggregated structure of long and irregular length. At higher magnification (×2000), the surface of the cellulose fiber was rough, and each fiber had a large diameter. After Cr(III)-catalyzed acid hydrolysis, the micro-sized fibers were disintegrated into individual, small fragments with reduced aggregated structure (Fig. 6b). Moreover, the nanocellulose showed a significant decrease in the diameter of the fibrils due to the delamination process, which further diminished intra- and intermolecular hydrogen bonding between cellulose polymers (Hamid *et al.* 2015). Similar findings have been reported previously (Hamid *et al.* 2014; Tan *et al.* 2015). FESEM measurements showed that the average diameter of nanocellulose decreased from 30.93 ± 10.85 μm to 15.15 ± 6.51 μm. Based on the TEM measurements (Fig. 6c), the nano-scale fibers were successfully isolated from micro-sized cellulose fibers. The nanocellulose fibers were conjoined in a web-like network with average diameters of 18.36 ± 7.34 nm, and the length of these fibers was hundreds to thousands of nanometers.

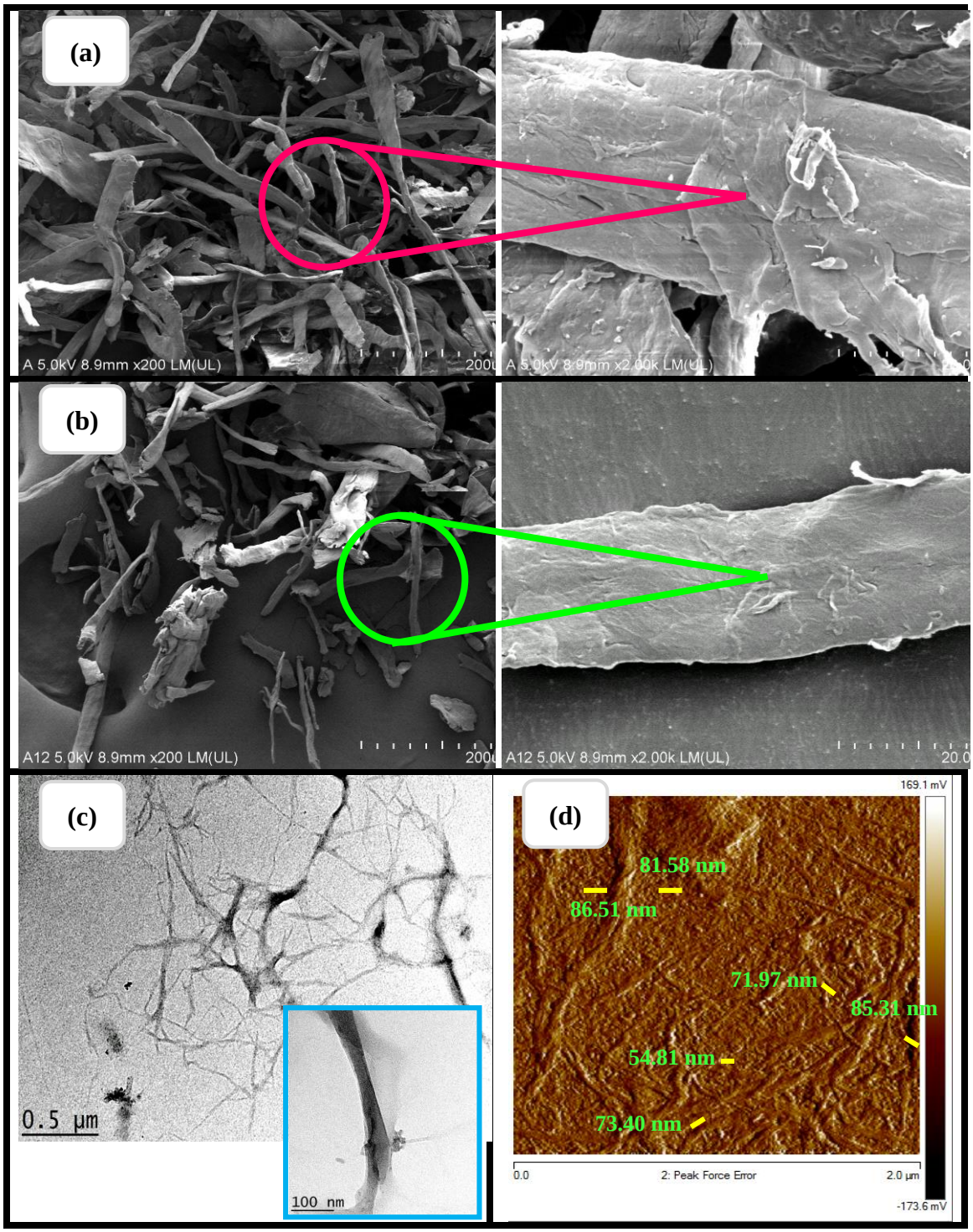


**Fig. 6.** FESEM images of (a) cellulose and (b) optimized nanocellulose; (c) TEM and (d) AFM images of optimized nanocellulose

The morphology and surface structures of optimized nanocellulose were further explained by AFM micrographs (Fig. 6d). The nature of the nanocellulose can be clearly seen by the enlarged AFM image. The AFM image further supports the conclusion that the nano-dimension cellulose was successfully hydrolyzed *via* $Cr(NO_3)_3$-catalyzed acid hydrolysis and was characterized by a short, thin, narrow whisker form. However, the

dimensions of nanocellulose observed by AFM were remarkably larger than TEM analysis; this difference was attributed to the different sample preparation methods as well as the fact that the samples were placed on different substrates, *i.e.*, a carbon-coated copper grid for TEM and a microscope slide for AFM (Feng *et al.* 2015).

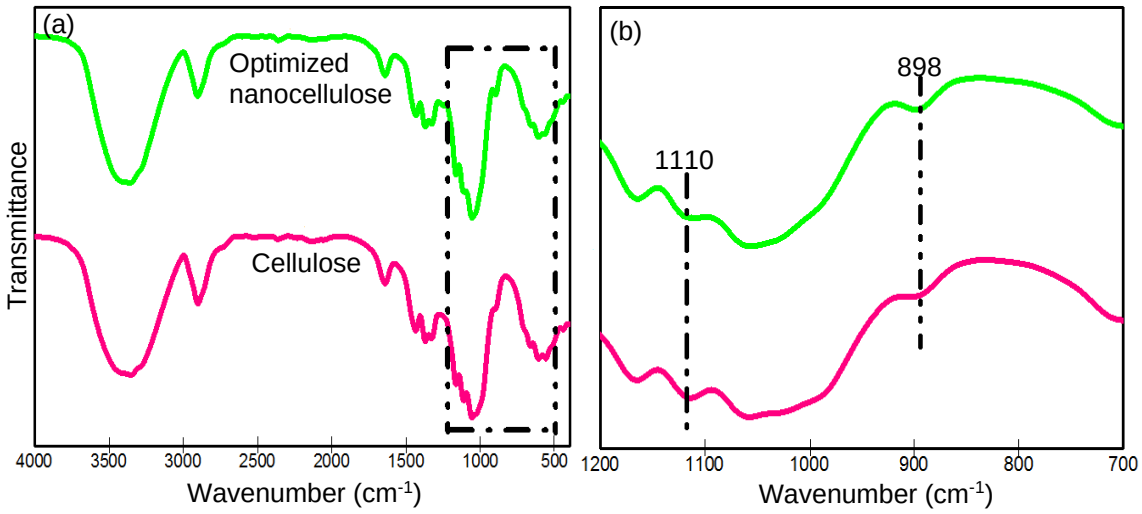


**Fig. 7.** (a) FTIR spectra of cellulose material and optimized nanocellulose and (b) enlargement of the spectral region of 1200 to 700 $cm^{-1}$, shown by dashed lines in (a) and (b)

*Chemical structural characterization by FT-IR analysis*

Fig. 7 shows the FTIR spectra of cellulose and nanocellulose prepared under optimal conditions. The broad peak observed at 3400 $cm^{-1}$ was attributed to the stretching vibration of O─H bonding from absorbed water molecules of the cellulose chains (Hou and Chen 2008; Jamshidi *et al.* 2015). In addition, C─H bond stretching vibration was assigned to the dominant peak near 2900 $cm^{-1}$ (Alemdar and Sain 2008). Two prominent peaks (1110 and 896 $cm^{-1}$) that correspond to the C─O─C pyranose ring skeletal vibration and *β*-linkages of $^4C_1$ ring confirmation, respectively, were observed. As reported by Chen *et al.* (2011), both of these peaks reflected the degree of polymerization in cellulose. For optimized nanocellulose, the peak at 1110 $cm^{-1}$ was less intense than in cellulose (Fig. 8b). This indicated that the degradation of glycosidic bonds that linked the *β*─D─glucopyranose monomers of the cellulose chains to produce nanocellulose (Kristensen *et al.* 2008). In contrast, the FTIR peak at 896 $cm^{-1}$, which was attributed to *β*─D─glucopyranosyl unit, was the similar in both samples, indicating that the cellulosic structure was retained after treatment (Li *et al.* 2009).

## CONCLUSIONS

1. RSM based on 5-level, 4-factor CCD was conducted to study the impact of catalytic acid hydrolysis factors and adjust the reaction temperature (30 to 100 °C), reaction time (0.5 to 2.5 h), $Cr(NO_3)_3$ concentration, and $H_2SO_4$ concentration (0.2 to 1.0 M) to optimize the crystallinity index and yield of nanocellulose.

2. As a hydrolysis catalyst, the $Cr(NO_3)_3$ metal salt enhanced the hydrolysis efficiency by improving the crystallinity index of yielded nanocellulose by 18.15%.
3. The hydrolysis process resulted in highly crystalline nanocellulose (85.35%) under a moderate temperature (82.2 °C) with small amounts of $Cr(NO_3)_3$ (0.22 M) and $H_2SO_4$ (0.80 M). A nanocellulose yield of 82.86% was obtained from the optimized reaction.
4. The average diameter of the optimized nanocellulose was 18.36 ± 7.34 nm.
5. The percentage error between the actual and predicted values of crystallinity index and nanocellulose yield was 0.316% and 0.531%, respectively. This result indicated that the developed empirical models were highly accurate, which verified that RSM analysis is a useful method for predicting and optimizing the reaction conditions for nanocellulose preparation via $Cr(NO_3)_3$-catalyzed selective acid hydrolysis.
6. The experimental parameters including reaction temperature, hydrolysis time, $Cr(NO_3)_3$ concentration and $H_2SO_4$ concentration had positive effect in enhancing the crystallinity of yielded optimized nanocellulose.

## ACKNOWLEDGMENTS

The authors are grateful for the financial support of the Minister of Science, Technology, and Innovation (MOSTI) e-Science Fund (SF002-2015) and the University of Malaya Postgraduate Research Grant Scheme PPP (PG063-2015A).

## REFERENCES CITED

Abd Hamid, S. B., Chowdhury, Z. Z., and Karim, M. Z. (2014). "Catalytic extraction of microcrystalline cellulose (MCC) from *Elaeis guineensis* using central composite design (CCD)," DOI: 10.15376/biores.9.4.7403-7426

Alemdar, A., and Sain, M. (2008). "Isolation and characterization of nanofibers from agricultural residues: Wheat straw and soy hulls," *Bioresource Technology*, 99(6), 1664-1671. DOI: 10.1016/j.biortech.2007.04.029

Azeredo, H. M. C., Imam, S. H., de Maria Figueirêdo, C. B., do Nascimento, D. M., and Rosa, M. F. (2015). "Nanocrystalline cellulose from coir fiber: Preparation, properties, and applications," in: *Handbook of Polymer Nanocomposites. Processing, Performance and Application, Volume C: Polymer Nanocomposites of Cellulose Nanoparticles*, Pandey, J. K., Reddy, K. R., Mohanty, A. K., and Misra, M. (eds.) Springer-Verlag, Berlin, Germany, pp. 15-26. DOI: 10.1007/978-3-642-45232-1_59

Boujemaoui, A., Mongkhontreerat, S., Malmström, E., and Carlmark, A. (2015). "Preparation and characterization of functionalized cellulose nanocrystals," *Carbohydrate Polymers* 115, 457-464. DOI: 10.1016/j.carbpol.2014.08.110

Chen, W., Yu, H., Liu, Y., Chen, P., Zhang, M., and Hai, Y. (2011). "Individualization of cellulose nanofibers from wood using high-intensity ultrasonication combined with chemical pretreatments," *Carbohydrate Polymers*, 83(4), 1804-1811. DOI: 10.1016/j.carbpol.2010.10.040

Feng, X., Meng, X., Zhao, J., Miao, M., Shi, L., Zhang, S., and Fang, J. (2015). "Extraction and preparation of cellulose nanocrystals from dealginate kelp residue:

structures and morphological characterization," *Cellulose* 22(3), 1763-1772. DOI: 10.1007/s10570-015-0617-z

Guo, J., Zhuang, Y., Chen, L., Liu, J., Li, D., and Ye, N. (2012). "Process optimization for microwave-assisted direct liquefaction of *Sargassum polycystum* C. Agardh using response surface methodology," *Bioresource Technology* 120, 19-25. DOI: 10.1016/j.biortech.2012.06.013

Hamid, S. B. A., Chowdhury, Z. Z., and Karim, M. Z. (2014). "Catalytic extraction of microcrystalline cellulose (MCC) from *Elaeis guineensis* using Central Composite Design (CCD)," *BioResources* 9(4), 7403-7426. DOI: 10.15376/biores.9.4.7403-7426

Hamid, S. B. A., Zain, S. K., Das, R., and Centi, G. (2015). "Synergic effect of tungstophosphoric acid and sonication for rapid synthesis of crystalline nanocellulose," *Carbohydrate Polymers* 138, 349-355. DOI: 10.1016/j.carbpol.2015.10.023

Hou, X. J., and Chen, W. (2008). "Optimization of extraction process of crude polysaccharides from wild edible BaChu mushroom by response surface methodology," *Carbohydrate Polymers* 72(1), 67-74. DOI: 10.1016/j.carbpol.2007.07.034

Jamshidi, M., Ghaedi, M., Dashtian, K., and Hajati, S. (2015). "New ion-imprinted polymer-functionalized mesoporous SBA-15 for selective separation and preconcentration of Cr(III) ions: Modeling and optimization," *RSC Advances* 5(128), 105789-105799. DOI: 10.1039/C5RA17873H

Karim, M. Z., Chowdhury, Z. Z., Hamid, S. B. A., and Ali, M. E. (2014). "Statistical optimization for acid hydrolysis of microcrystalline cellulose and its physiochemical characterization by using metal ion catalyst," *Materials* 7(10), 6982-6999. DOI: 10.3390/ma7106982

Kopania, E., Wietecha, J., and Ciechańska, D. (2012). "Studies on isolation of cellulose fibres from waste plant biomass," *Fibres & Textiles in Eastern Europe* 6B(96), 167-172.

Kristensen, J. B., Thygesen, L. G., Felby, C., Jørgensen, H., and Elder, T. (2008). "Cell-wall structural changes in wheat straw pretreated for bioethanol production," *Biotechnology for Biofuels* 1(5), 1-9. DOI: 10.1186/1754-6834-1-5

Li, J., Qiang, D., Zhang, M., Xiu, H., and Zhang, X. (2015). "Joint action of ultrasonic and $Fe^{3+}$ to improve selectivity of acid hydrolysis for microcrystalline cellulose," *Carbohydrate Polymers* 129, 44-49. DOI: 10.1016/j.carbpol.2015.04.034

Li, J., Xiu, H., Zhang, M., Wang, H., Ren, Y., and Ji, Y. (2013). "Enhancement of cellulose acid hydrolysis selectivity using metal ion catalysts," *Current Organic Chemistry* 17(15), 1617-1623. DOI: 10.2174/13852728113179990071

Li, J., Zhang, X., Zhang, M., Xiu, H., and He, H. (2014). "Optimization of selective acid hydrolysis of cellulose for microcrystalline cellulose using $FeCl_3$," *BioResources* 9(1), 1334-1345. DOI: 10.15376/biores.9.1.1334-1345

Li, R., Fei, J., Cai, Y., Li, Y., Feng, J., and Yao, J. (2009). "Cellulose whiskers extracted from mulberry: A novel biomass production," *Carbohydrate Polymers* 76(1), 94-99. DOI: 10.1016/j.carbpol.2008.09.034

Li, W., Yue, J., and Liu, S. (2012). "Preparation of nanocrystalline cellulose *via* ultrasound and its reinforcement capability for poly(vinyl alcohol) composites," *Ultrasonics Sonochemistry* 19(3), 479-485. DOI: 10.1016/j.ultsonch.2011.11.007

Liew, S. Y., Thielemans, W., and Hewakandamby, B. (2016). "Separation of sulphuric acid from an acid suspension of cellulose nanocrystals by manual shaking," *Journal of Nano Research* 38, 58-72. DOI: 10.4028/www.scientific.net/JNanoR.38.58

Liu, H., Liu, D., Yao, F., and Wu, Q. (2010). "Fabrication and properties of transparent polymethylmethacrylate/cellulose nanocrystals composites," *Bioresource Technology* 101(14), 5685-5692. DOI: 10.1016/j.biortech.2010.02.045

Lu, Q., Tang, L., Lin, F., Wang, S., Chen, Y., Chen, X., and Huang, B. (2014). "Preparation and characterization of cellulose nanocrystals via ultrasonication-assisted $FeCl_3$-catalyzed hydrolysis," *Cellulose* 21(5), 3497-3506. DOI: 10.1007/s10570-014-0376-2

Mohan, S., Viruthagiri, T., and Arunkumar, C. (2014). "Statistical optimization of process parameters for the production of tannase by *Aspergillus flavus* under submerged fermentation," *3 Biotech* 4(2), 159-166. DOI: 10.1007/s13205-013-0139-z

Olsson, C., and Westman, G. (2013). "Direct dissolution of cellulose: Background, means and applications," in: *Cellulose- Fundamental Aspects*, van de Ven, T., and Godbout, L. (eds.), InTech, Rijeka, Croatia, pp. 144-178.

Pandey, J. K., Ahn, S. H., Lee, C. S., Mohanty, A. K., and Misra, M. (2010). "Recent advances in the application of natural fiber based composites," *Macromolecular Materials and Engineering* 295(11), 975-989. DOI: 10.1002/mame.201000095

Peng, L., Lin, L., Zhang, J., Zhuang, J., Zhang, B., and Gong, Y. (2010). "Catalytic conversion of cellulose to levulinic acid by metal chlorides," *Molecules* 15(8), 5258-72. DOI: 10.3390/molecules15085258

Segal, L., Creely, J., Martin, A., and Conrad, C. (1959). "An empirical method for estimating the degree of crystallinity of native cellulose using the X-ray diffractometer," *Textile Research Journal* 29(10), 786-794. DOI: 10.1177/004051755902901003

Tan, X. Y., Abd Hamid, S. B., and Lai, C. W. (2015). "Preparation of high crystallinity cellulose nanocrystals (CNCs) by ionic liquid solvolysis," *Biomass and Bioenergy* 81, 584-591. DOI: 10.1016/j.biombioe.2015.08.016

Tang, L. R., Huang, B., Ou, W., Chen, X. R., and Chen, Y. D. (2011). "Manufacture of cellulose nanocrystals by cation exchange resin-catalyzed hydrolysis of cellulose," *Bioresource Technology* 102(23), 10973-10977. DOI: 10.1016/j.biortech.2011.09.070

Yahya, M. B., Lee, H. V., and Hamid, S. B. A. (2015). "Preparation of nanocellulose via transition metal salt-catalyzed hydrolysis pathway," *BioResources* 10(4), 7627-7639. DOI: 10.15376/biores.10.4.7627-7639

Zhao, H., Holladay, J. E., Brown, H., and Zhang, Z. C. (2007). "Metal chlorides in ionic liquid solvents convert sugars to 5-hydroxymethylfurfural," *Science* 316(5831), 1597-1600. DOI: 10.1126/science.1141199

Zhao, J., Zhang, H., Zheng, R., Lin, Z., and Huang, H. (2011). "The enhancement of pretreatment and enzymatic hydrolysis of corn stover by $FeSO_4$ pretreatment," *Biochemical Engineering Journal* 56(3), 158-164. DOI: 10.1016/j.bej.2011.06.002

Article submitted: January 28, 2016; Peer review completed: March 18, 2016; Revised version received: March 24, 2016; Accepted: April 1, 2016; Published: April 12, 2016.
DOI: 10.15376/biores.11.2.4645-4662